Supporting Information

Pyrolysis-Driven Synthesis of Nanoscale Carambola-Like Carbon Decorated with Atomically Dispersed Fe Sites toward Efficient Oxygen Reduction Reaction

Hongsa Han, Yunlong Zhang, Yuanyuan Cong, Jiaqi Qin, Zihui Zhai, Xueliang Wang, Rui Gao, Guanghui Zhang, Xinwen Guo and Yujiang Song*

State Key Laboratory of Fine Chemicals, School of Chemical Engineering, Dalian University of Technology, Dalian 116024, China.

Experimental

Chemicals

Tetrakis(4-carboxyphenyl) porphyrin (H_2TCPP, >97%,) was purchased from Macklin Biochemical Co., Ltd. (Shanghai, China). $ZrCl_4$ (analytical grade) was purchased from Aladdin Bio-Chem Technology Co., Ltd. (Shanghai, China). Other chemicals are analytical grade and purchased from Sinopharm Chemical Reagent Co., Ltd. (Beijing, China). All the chemicals were used as received without further purification. Ultrapure water (18.2 MΩ cm at 25 °C) was obtained from Millipore water system (Synergy UV, France).

Synthesis of FeTCPP

Typically, H_2TCPP (1.0 mmol) and $FeCl_3$ (15.0 mmol) were dissolved in N, N-dimethylformamide (DMF) (200 mL), and the mixture was refluxed for 6 h. After cooling down to room temperature, H_2O (300 mL) was added. The purple precipitates were collected by filtration and washed with H_2O twice. Accornding to mass spectrometry (MS), we have successfully synthesized Fe^{III} tetrakis(4-carboxyphenyl) porphyrin (FeTCPP) (Figure S1). After the coordination of Fe^{III} with H_2TCPP, the four Q band (500-750 nm) peaks of H_2TCPP have been converted into two peaks due to the improvement of the macrocyclic molecular symmetry (Figure S2).

Synthesis of PCN-222 nanocapsules

Typically, 8.33 mg $ZrCl_4$, 205 mg benzoic acid, and 166 μL H_2O were dissolved in 1.66 mL DMF under magnetic stirring for 5 minutes in a 10 mL pyrex vial. Next, 8.33 mg FeTCCP was added in the above-mentioned solution and keeped magnetic stirring for 10 minutes at room temperature. Then, the resulting homogeneous solution was heated at 120°C for 8 h. The black precipitates were separated via centrifugation at 4000 rpm for 5 minutes and further purified with DMF and ethanol for several times. The obtained dark-green powder was dried

at 65 °C for 24 h. Additional synthetic detail is summarized in Table S1 for varying the length and the width of PCN-222.

Synthesis of nanocarambola electrocatalysts

Typically, the pyrolysis of PCN-222 nanocapsules was carried out in Ar in a temperature-programmable tube furnace by ramping up temperature from room temperature to 600, 650, 700, 750, 800 and 900 °C, respectively, at a heating rate of 5 °C min^{-1}, and held at each targeted temperature for 2 h. Subsequently, identified optimal sample was pickled in 20 wt% HF aqueous solution for 6 h at 60 °C to remove ZrO_2 and other unstable by-products. The black sample was collected by centrifugation, washed several times with distilled water and ethanol, and dried at 60 °C under vacuum overnight.

Characterizations

Transmission electron microscopy (TEM) images were taken on JEM-2100 microscope (Japan Electronics, Japan) operated at 200 KeV. High-resolution transmission electron microscopy (HRTEM) images and elemental mappings were recorded on a FEI Tecnai G2 F30 S-Twin microscope (FEI, US) operated at 300 KeV. High-angle annular dark-field scanning TEM (HAADF-STEM) images were recorded on a JEOL JEM-ARM200F microscope (Japan Electronics, Japan). Scanning electron microscopy (SEM) was carried out on a Field Emission Scanning Electron Microscope (NOVA NanoSEM 450) (FEI, US). X-ray diffraction (XRD) patterns were collected on a Rigaku Smart lab 9 diffractometer with a Cu Kα radiation source (Rigaku, Japan). X-ray photo-electron spectroscopy (XPS) measurements were performed on a Thermo ESCALAB250Xi spectrometer using monochromatic Al Kα line (1486.6 eV) as the X-ray source (Thermo, US). Inductively coupled plasma-optical emission spectroscopy (ICP-OES) was carried out on a PerkinElmer ICP-OES 7300DV (PerkinElmer, US). Elemental analysis was performed on a Soriba EMDA-930 oxygen, nitrogen, hydrogen analyzer. Nitrogen adsorption/desorption curves were measured at 77 K on a Quantachrome Quadrasorb-SI Analyzer (Quantachrome, US), where Brunauer-Emmett-

Teller (BET) method was used for surface area determination. MS was carried out on MALDI micro MX (Waters, US). UV-Vis spectra were conducted by using a Specord S600 spectrophotometer (Analytic Jena, Germany). X-ray absorption fine structure spectra (Fe K-edge) were collected at BL14W beamline of Shanghai Synchrotron Radiation Facility (SSRF) installed with a Si (111) double-crystal monochromator. The storage rings of SSRF were operated at 3.5 GeV with a constant current of 200 mA. The data collection was carried out in fluorescence mode via a Lytle detector. ^{57}Fe Mössbauer spectroscopy was performed on MFD-500AV-02 (Topologic Systems, Japan) at room temperature. A ^{57}Co (Rh) source with a constant acceleration mode was used as the radioactive source. The ^{57}Fe Mössbauer spectra were fitted with the MossWinn computer program.

Electrochemical measurements

Electrochemical measurements were carried out on CHI 760D electrochemical workstation (CH Instruments, Shanghai, China) in a three-electrode electrochemical cell with a glassy carbon rotating disk electrode (RDE) or rotating ring-disk electrode (RRDE) as the working electrode, a graphite rod as the counter electrode, and Hg/HgO as the reference electrode in alkaline solution, or a saturated calomel electrode (SCE) as the reference electrode in acidic solution that is connected to the cell by a salt bridge (agar gel containing saturated KNO_3). All potentials in this study were referred to that of reversible hydrogen electrode (RHE). A 5.0 mm diameter of glassy carbon disk (0.19625 cm^2, PINE) and a 5.0 mm diameter of glassy carbon disk (0.19625 cm^2, PINE) with Pt ring (0.1099 cm^2, 6.5 mm inner-diameter and 7.5 mm outer-diameter) were used in RDE and RRDE experiments, respectively.

Typically, the electrocatalyst ink (2 mg mL^{-1}) was prepared by blending certain amount of electrocatalyst with water, ethanol, and Nafion perfluorinated resin solution (V_{water}:$V_{ethanol}$:V_{Nafion} = 1:9:0.06) under sonication for 2 min. The suspension was pipetted onto the RDE or the RRDE and evaporated in air, resulting in an electrocatalyst loading of

0.4-1.0 mg cm^{-2}. For comparison, commercial 20 wt% Pt/C ink (1 mg mL^{-1}) was prepared in a similar manner, and the Pt/C loading was 10 μg_{Pt} cm^{-2} in acidic solution, and 20 μg_{Pt} cm^{-2} in alkaline solution. All RDE and RRDE tests were carried out at 25 °C in N_2-saturated and O_2-saturated 0.1 mol L^{-1} $HClO_4$ or KOH aqueous solution. ORR polarization curves were obtained at a rotation rate of 1600 rpm and a positive scan rate of 10 mV s^{-1}. The ring potential of RRDE was set to 1.2 V (vs. RHE). Peroxide species yield (H_2O_2 % in acidic solution, and HO_2^- % in alkaline solution) and electron transfer number (N) were evaluated based on the following equations：

$$H_2O_2\% = \frac{200I_R/n}{I_D + I_R/n} \quad (1)$$

$$N = 4 \times \frac{I_D}{I_D + I_R/n} \quad (2)$$

Where I_D is the Faradaic current at the disk, I_R is the Faradaic current at the ring and n is the H_2O_2/HO_2^- collection coefficient (25.6%) at the ring. For accelerated durability test, potential cycling was conducted between 0.6-1.2 V (vs. RHE) in acidic or alkaline solution at a scan rate of 100 mV s^{-1} for a total number of 2500 cycles in O_2-saturated electrolyte that can provide a harsh degradation condition. Meanwhile, ORR polarization curves were collected at certain cycles to track the degradation of the electrocatalysts.

Figures

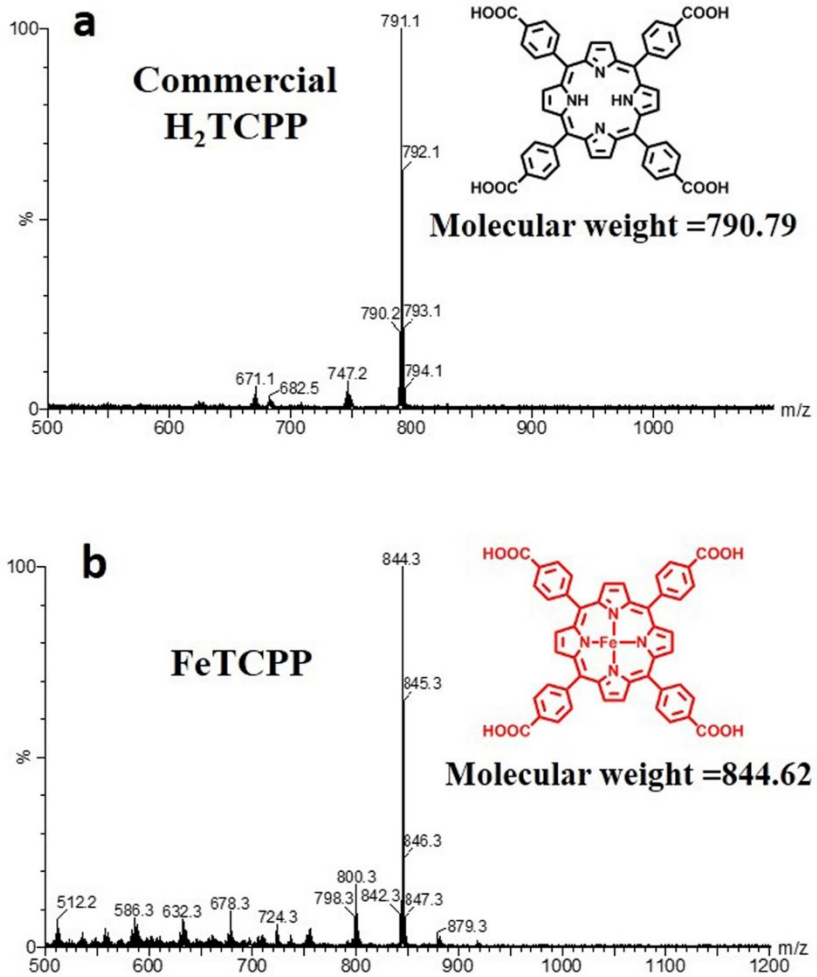

Figure S1. (a) MS of commercial H_2TCPP with molecular structure and weight; (b) MS of house-made FeTCPP with molecular structure and weight.

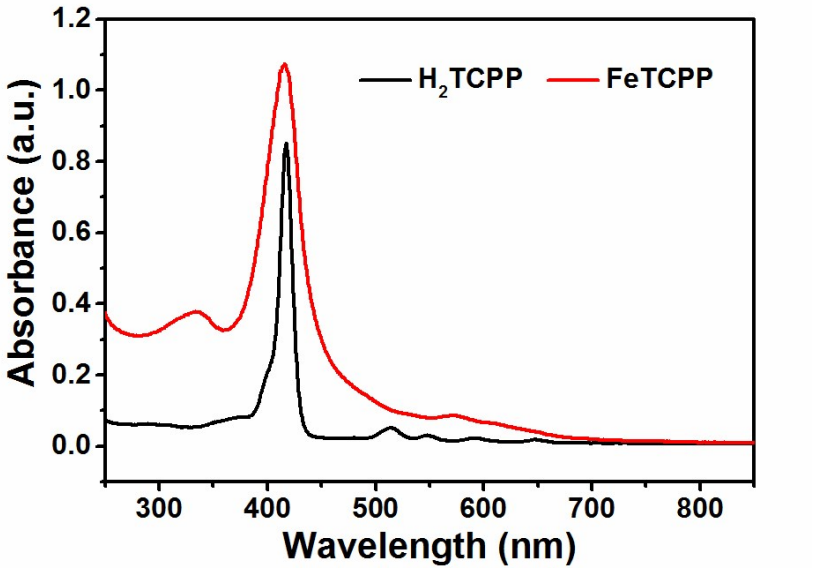

Figure S2. UV-Vis spectra of H_2TCPP and house-made FeTCPP.

Table S1. Synthetic parameters and corresponding average length and width of nanocapsules

Sample	Benzoic acid (mg)	FeTCCP (mg)	$ZrCl_4$ (mg)	DMF (mL)	H_2O (mL)	Length (nm)	Width (nm)
PCN-222 nanocapsules	75	8.33	8.33	1.66	0.1666	75±10	50±5
	105	8.33	8.33	1.66	0.1666	170±20	100±15
	135	8.33	8.33	1.66	0.1666	350±50	160±20
	205	8.33	8.33	1.66	0.1666	720±80	320±30
	235	8.33	8.33	1.66	0.1666	1200±100	450±40

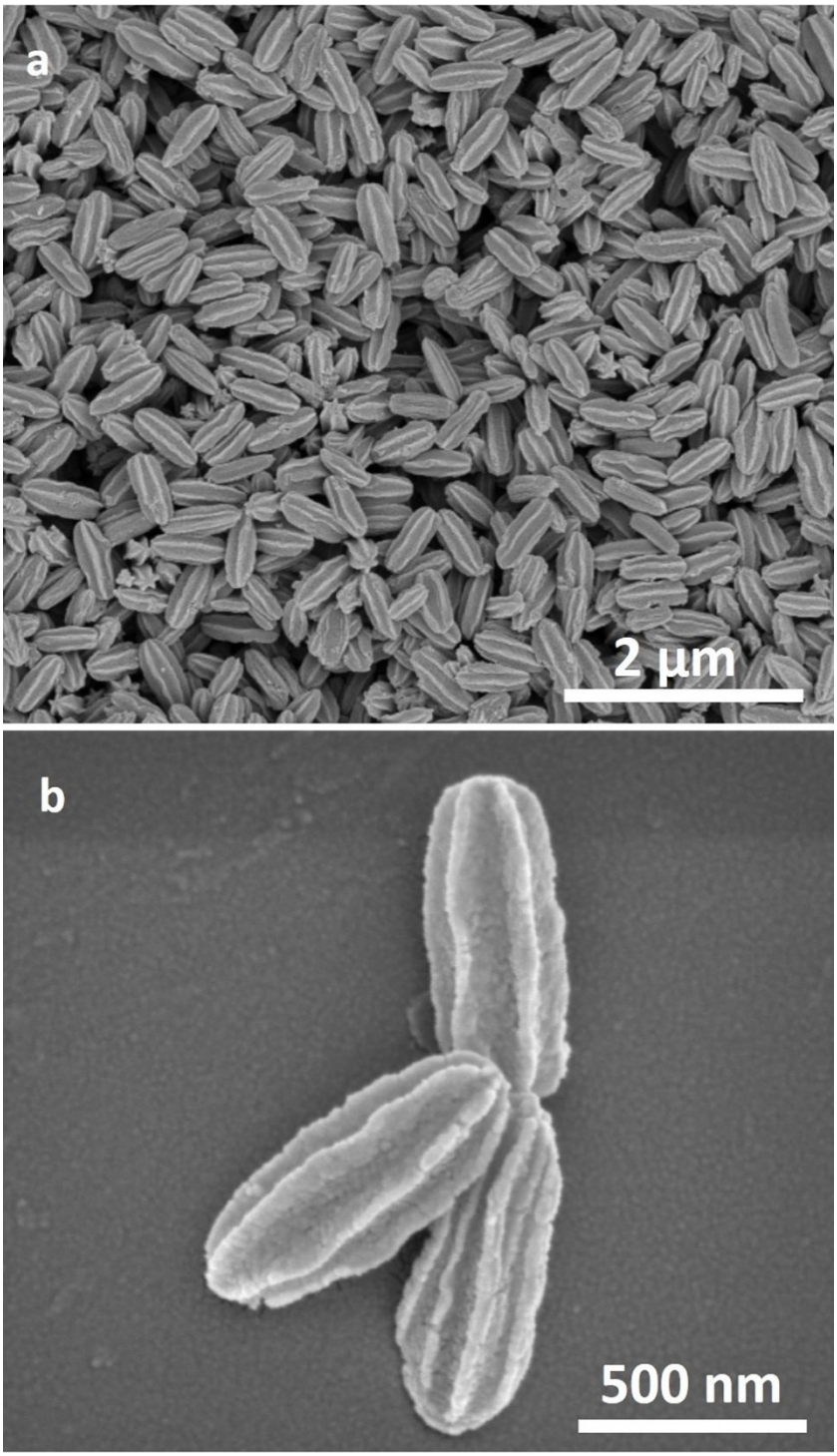

Figure S3. (a-b) SEM images of nanocarambolas at different magnifications before HF leaching.

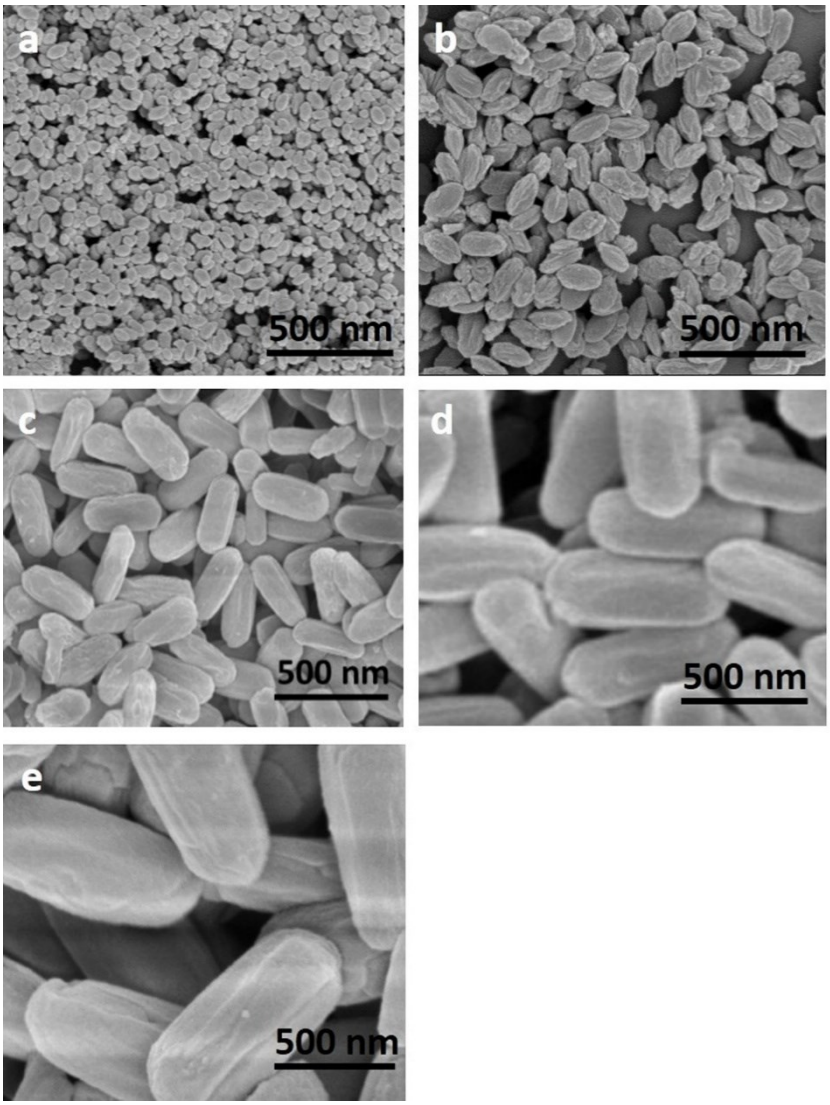

Figure S4. (a-e) SEM images of PCN-222 nanocapsules with different lengths and widths.

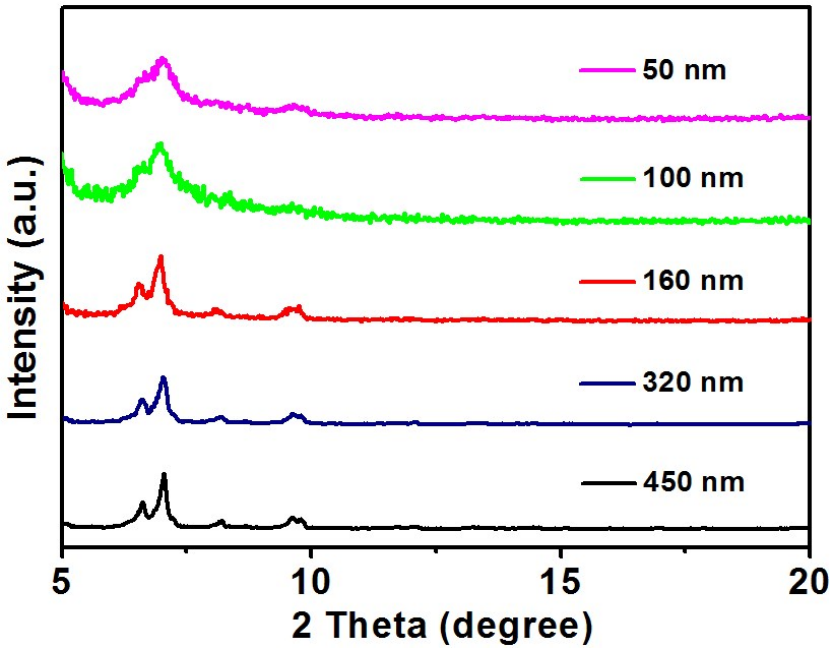

Figure S5. XRD patterns of PCN-222 nanocapsules with different average widths. (Note: the length is omitted for simplicity.)

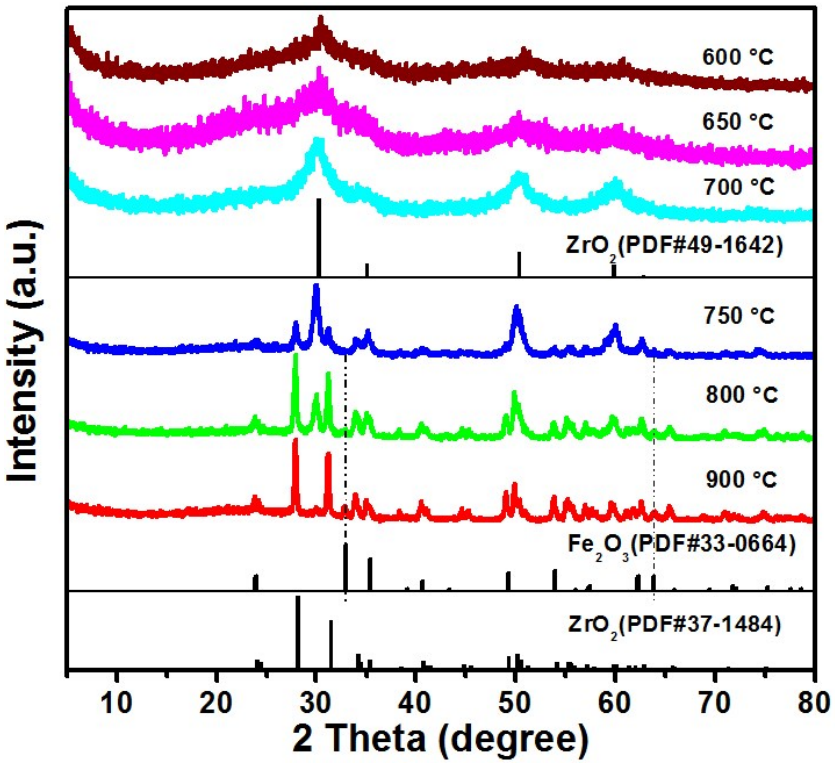

Figure S6. XRD patterns of pyrolitic nanocapsules obtained at different pyrolysis temperatures with nanocapsules at an average length of 750 nm and width of 320 nm as an example.

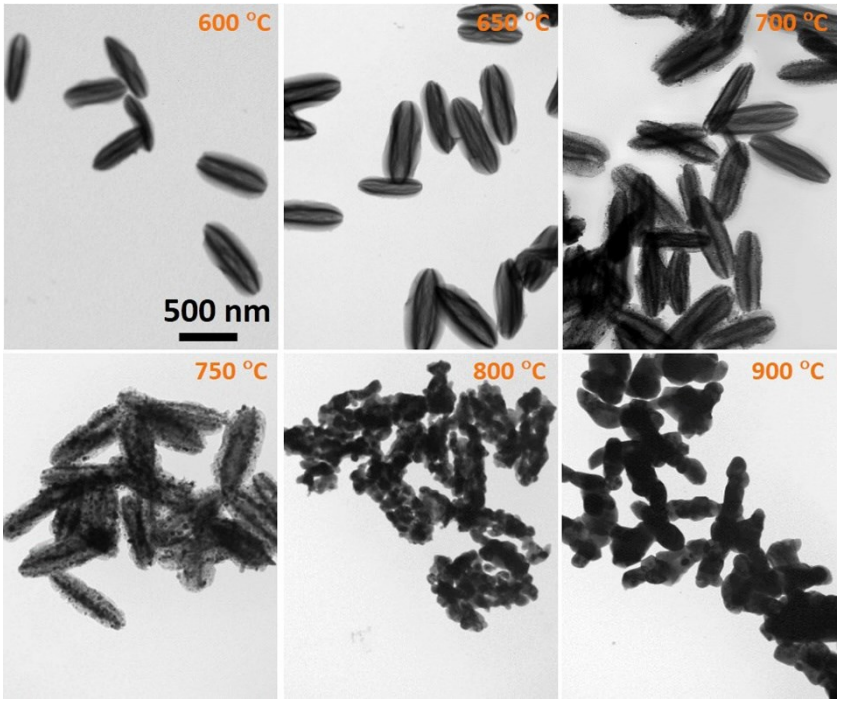

Figure S7. TEM images of pyrolitic nanocapsules obtained at different pyrolysis temperatures with nanocapsules at an average length of 750 nm and width of 320 nm as an example.

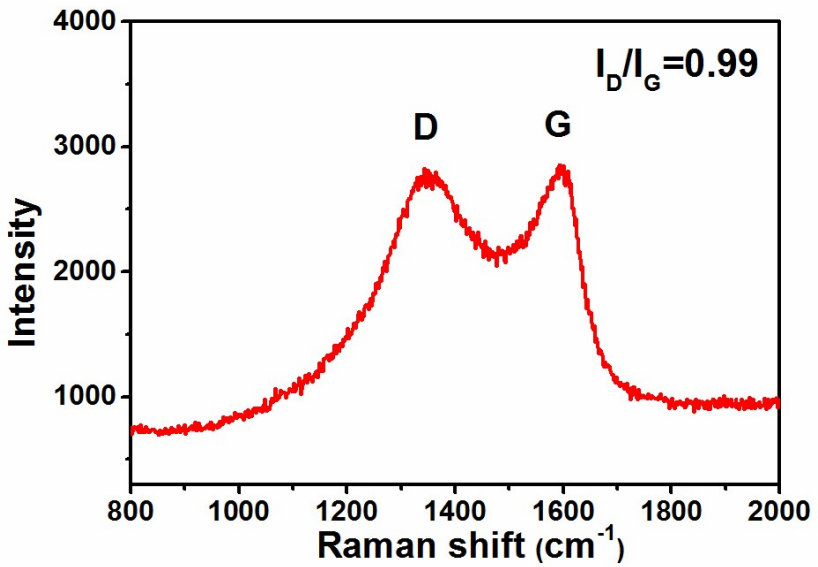

Figure S8. Raman spectrum of pyrolytic nanocapsules at an average length of 720 nm and width of 320 nm obtained by pyrolysis at 700 °C before HF leaching.

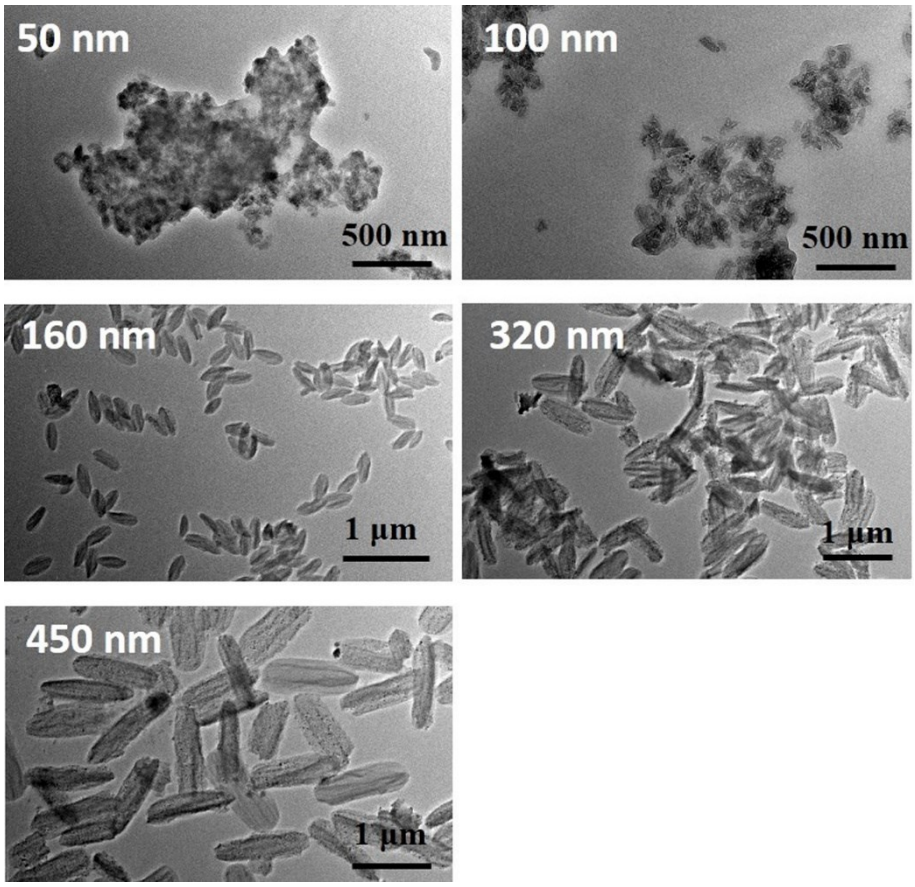

Figure S9. TEM images of pyrolytic nanocapsules with different average widths obtained at 700 °C. (Note: the average length is omitted for simplicity.)

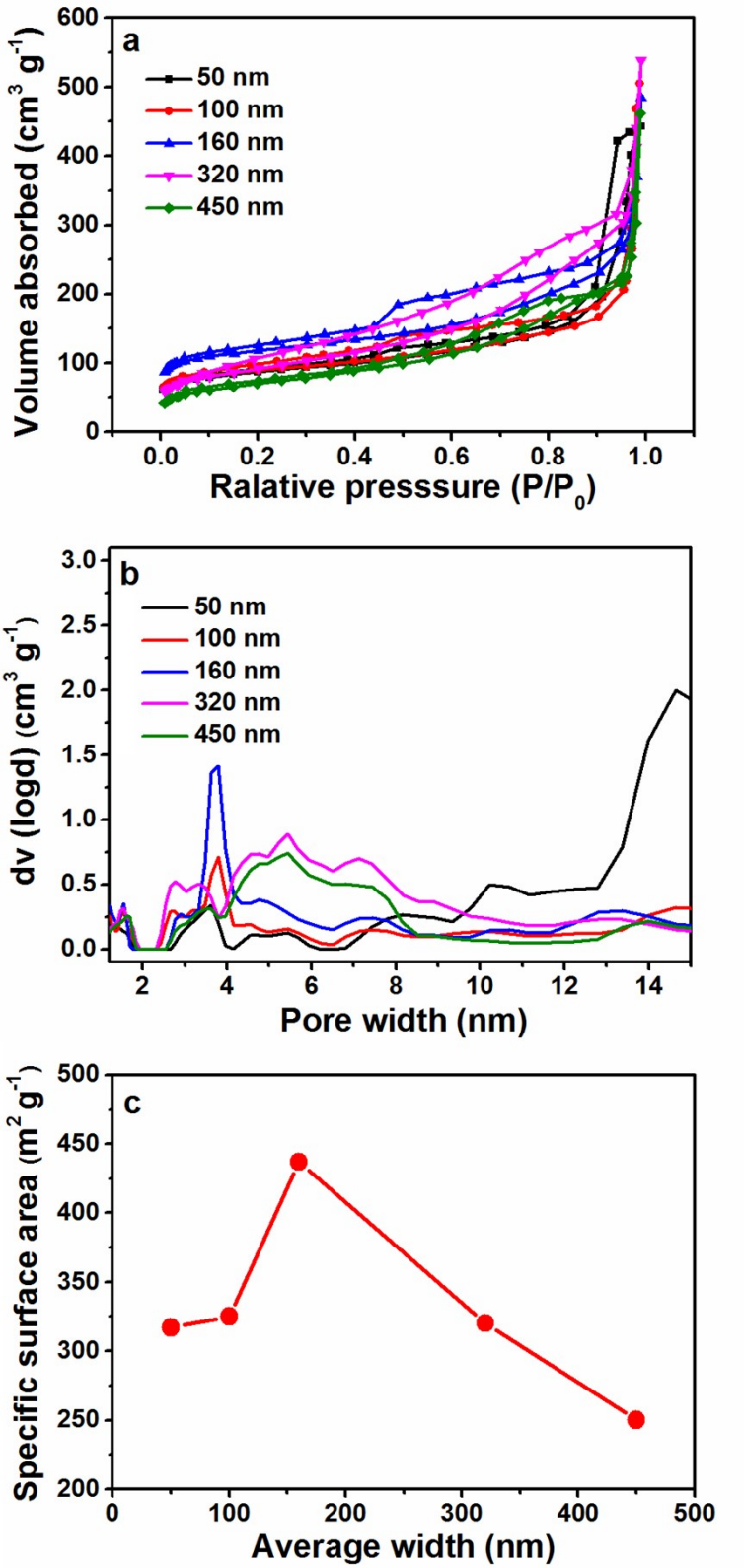

Figure S10. (a) Nitrogen adsorption/desorption isotherms of pyrolytic nanocapsules with different average widths from 50 to 450 nm heat-treated at 700 °C; (b) corresponding pore size distribution; (c) the correlation plot between the average width of nanocapsules and the specific surface areas of the pyrolytic nanocapsules.

Table S2. BET surface area, total pore volume, and micropore volume of the pyrolytic nanocapsules with different average widths heat-treated at 700 °C

The average width of nanocapsules (nm)	Surface area (m^2 g^{-1})	Total pore volume (cm^3 g^{-1})	Micropore volume (cm^3 g^{-1})
50	317.5	0.67	0.069
100	325.9	0.78	0.071
160	437.8	0.75	0.102
320	326.3	0.83	0.020
450	250.6	0.72	0.017

Note: The average length is omitted for simplicity.

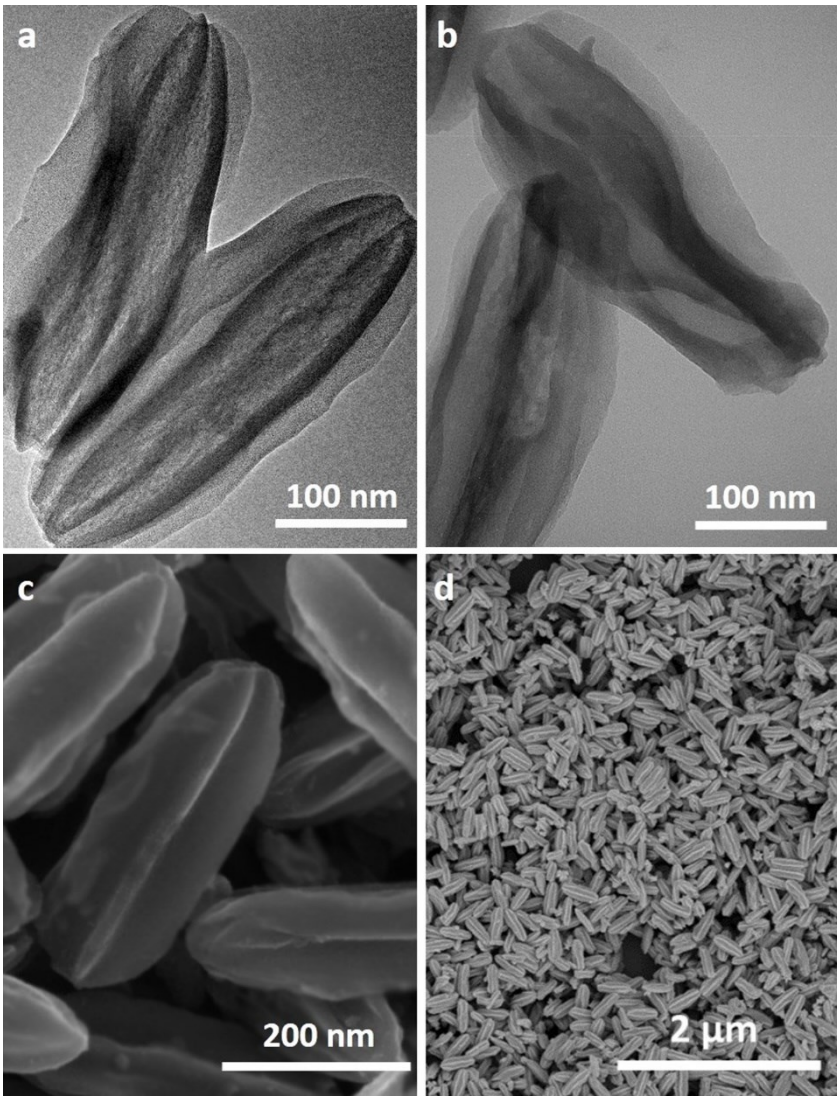

Figure S11. (a) TEM image of nanocarambolas befor HF leaching; (b) TEM image of nanocaramblolas after HF leaching; (c-d) SEM images of nanocarambolas at different magnifications after HF leaching. The nanocarambolas were synthesized with the nanocapsules in an average length of 350 nm and width of 160 nm at 700 °C.

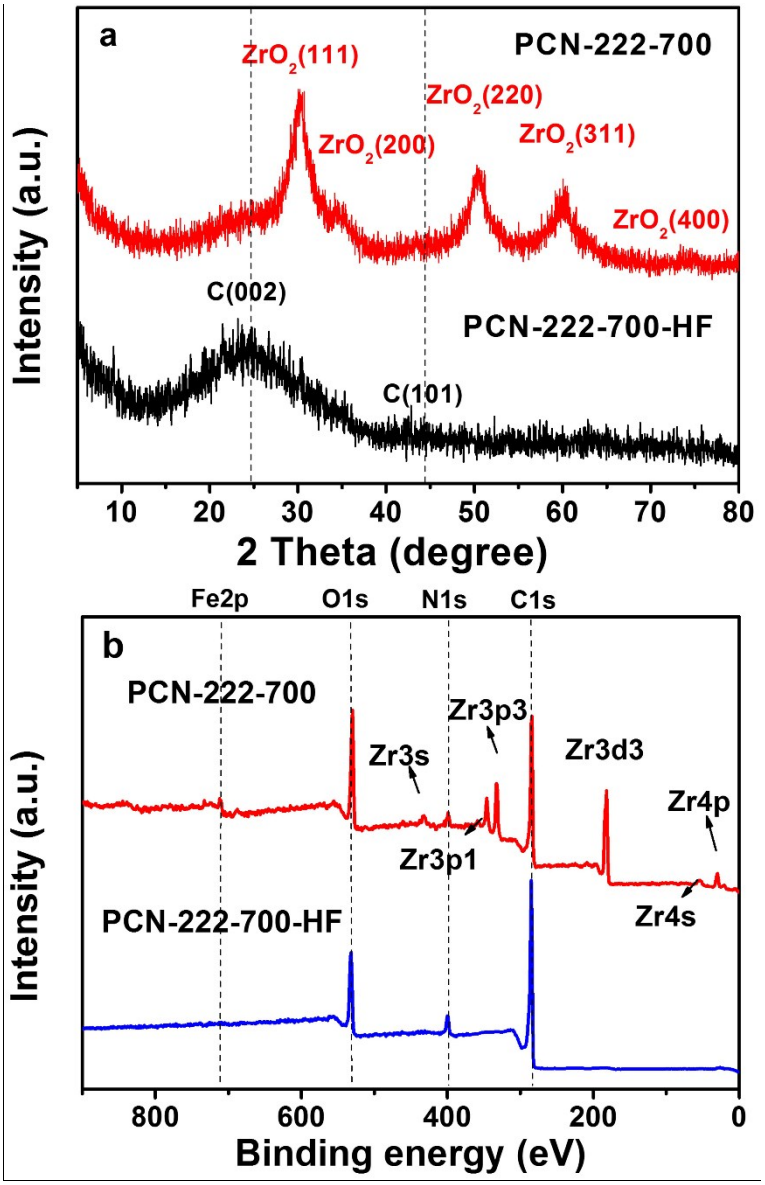

Figure S12. (a) XRD patterns and (b) XPS spectra of PCN-222-700 and PCN-222-700-HF.

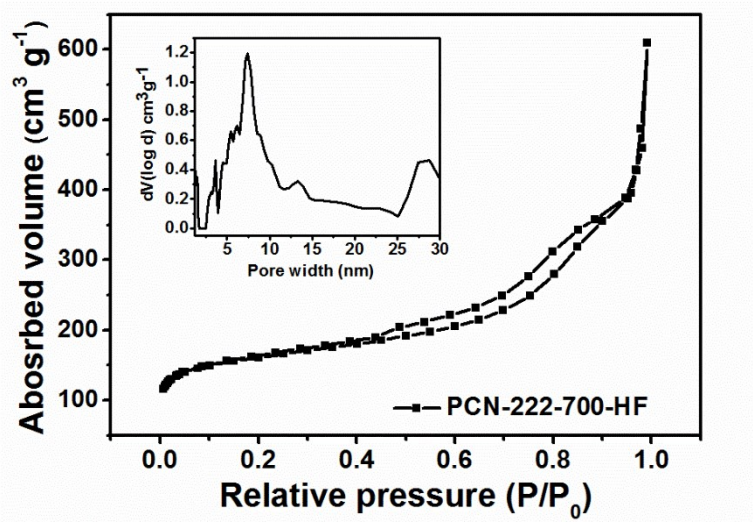

Figure S13. Nitrogen adsorption/desorption isotherm of PCN-222-700-HF. (Inset: the corresponding pore size distribution.)

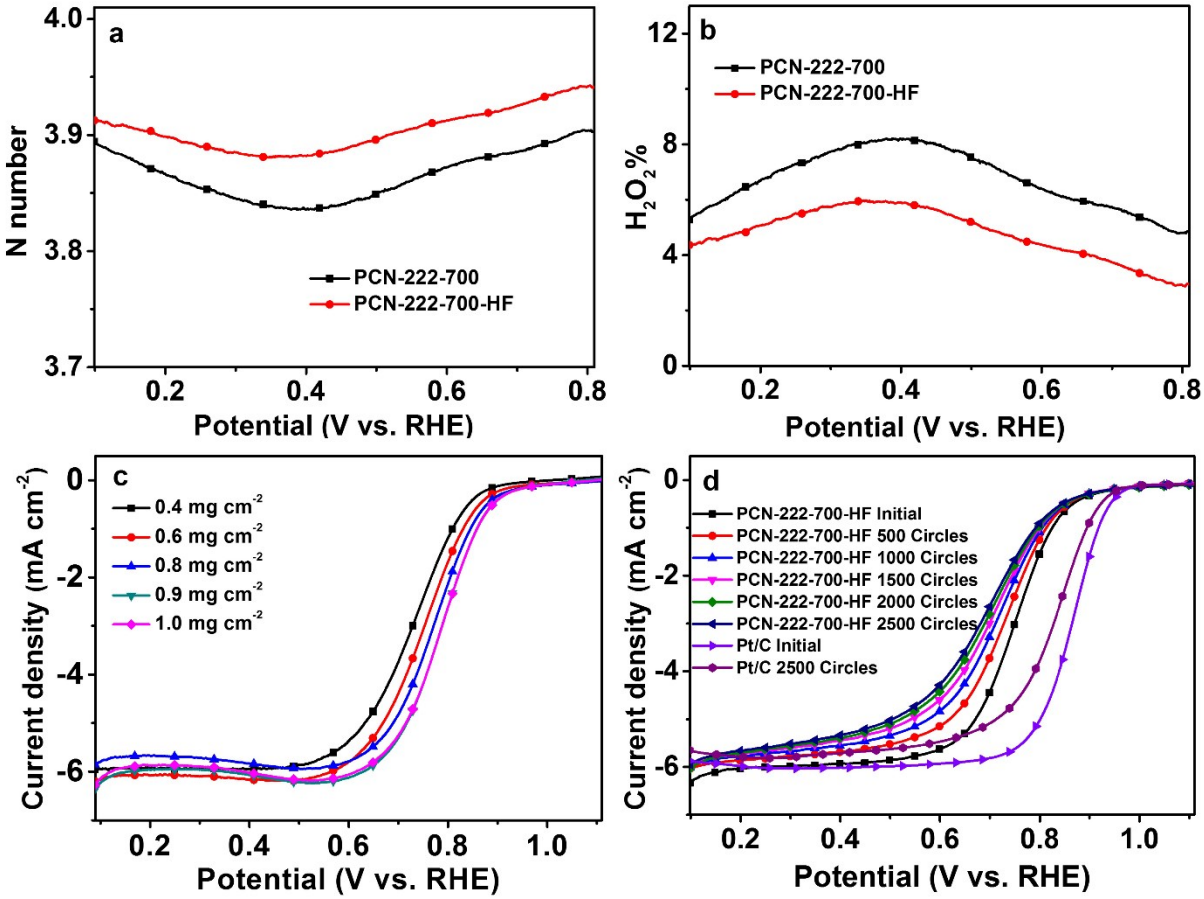

Figure S14. (a) Electron transfer number N and (b) H_2O_2 yield of PCN-222-700 and PCN-222-700-HF; (c) ORR polarization curves of PCN-222-700-HF with different electrocatalyst loadings (0.4-1.0 mg cm^{-2}) on RDE; (d) accelerated durability test of PCN-222-700-HF and commercial Pt/C (10 μg_{Pt} cm^{-2}). (Note: ORR polarization curves were recorded at a positive sweep rate of 10 mV s^{-1} and 1600 rpm in 0.1 mol L^{-1} $HClO_4$.)

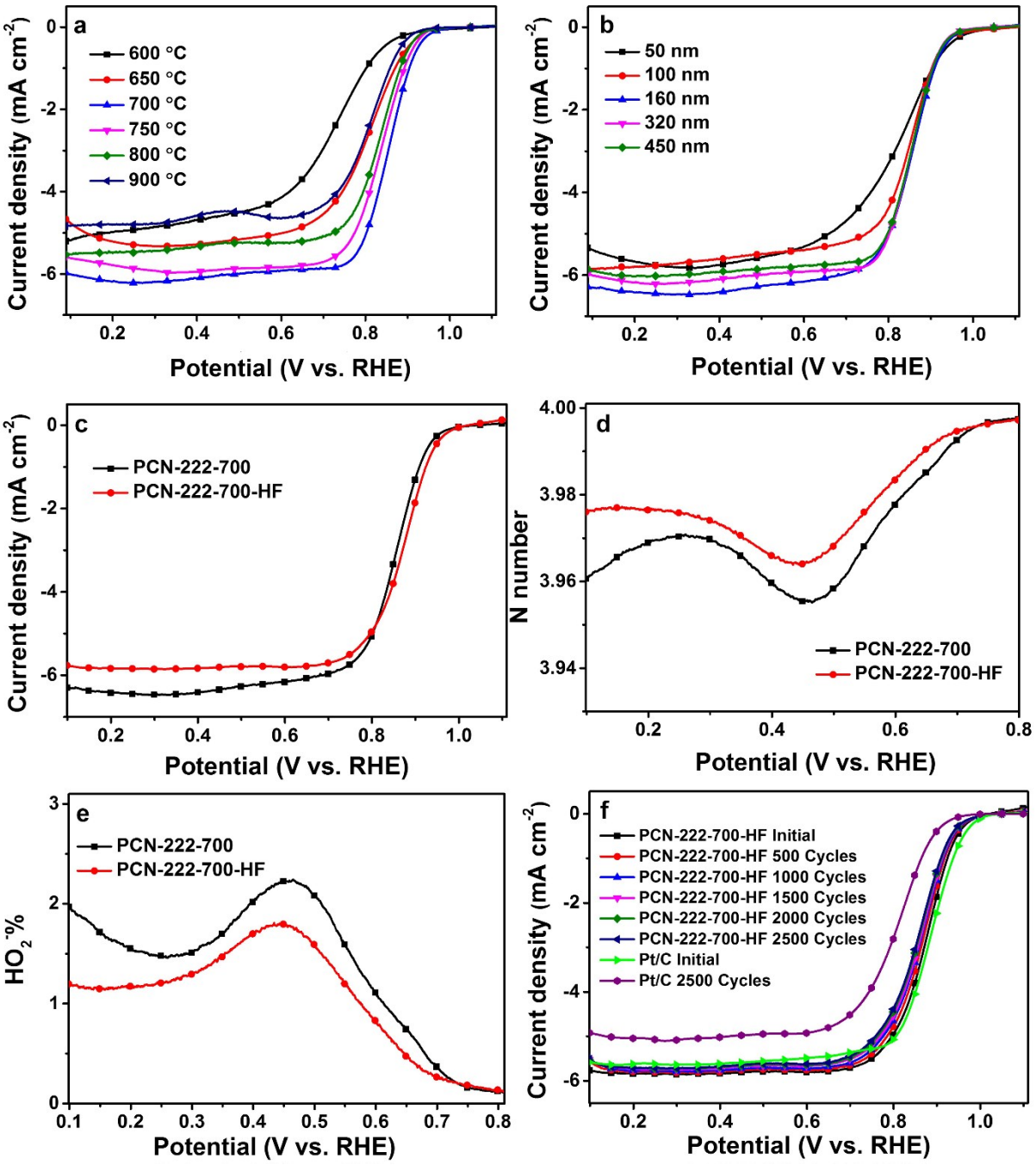

Figure S15. (a) ORR polarization curves of pyrolytic nanocapsules at different pyrolysis temperatures with nanocapsules in an average length of 720 nm and width of 320 nm as an example; (b) ORR polarization curves of pyrolytic nanocapsules with different average widths heat-treated at 700 °C; (c) ORR polarization curves of PCN-222-700 and PCN-222-700-HF; (d) electron transfer number N of PCN-222-700 and PCN-222-700-HF; (e) HO_2^- yield of PCN-222-700 and PCN-222-700-HF; (f) accelerated durability test of PCN-222-700-HF and commercial Pt/C. (Note: the average length is omitted for simplicity in (b); ORR curves were recorded at a positive sweep rate of 10 mV s^{-1} and 1600 rpm in 0.1 mol L^{-1} KOH aqueous solution.)

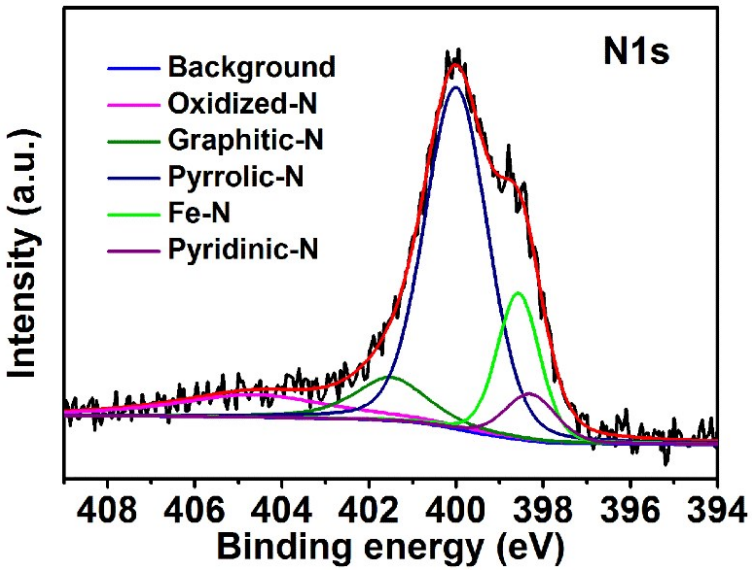

Figure S16. High-resolution N1s XPS of PCN-222-700-HF.

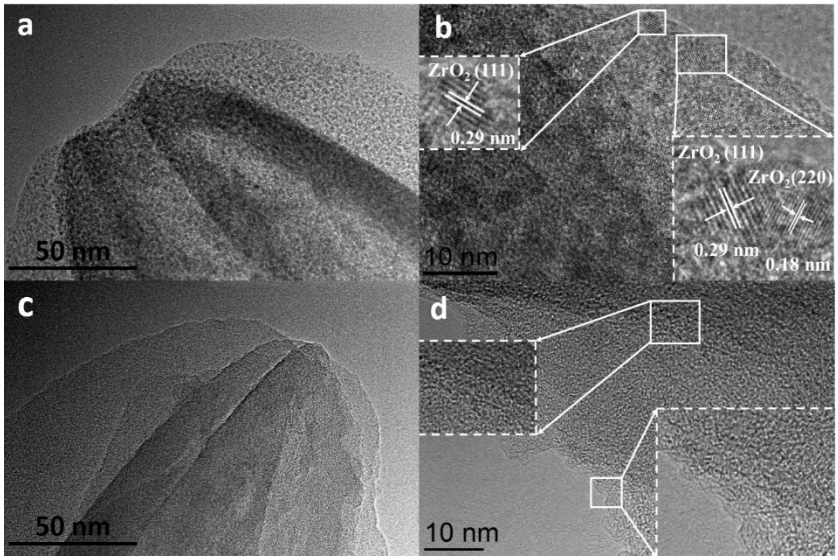

Figure S17. (a) TEM image of PCN-222-700; (b) HRTEM image of PCN-222-700; (c) TEM image of PCN-222-700-HF; (d) HRTEM image of PCN-222-700-HF. Insets in (b): selected ZrO_2 nanoparticles with lattice fringes; Insets in (d): selected area without lattice fringe.

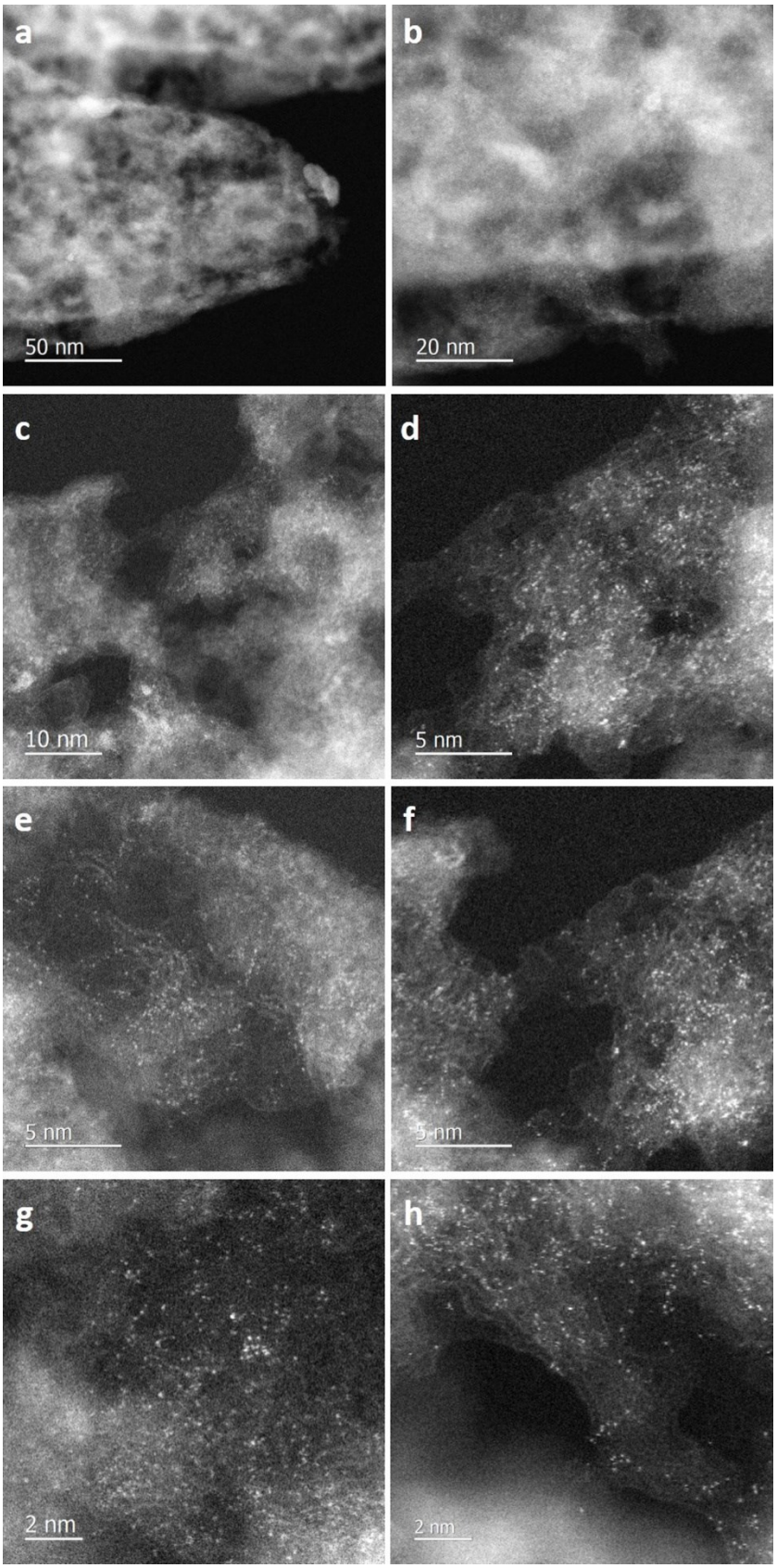

Figure S18. (a-h) HAADF-STEM images of PCN-222-700-HF at different magnifications.

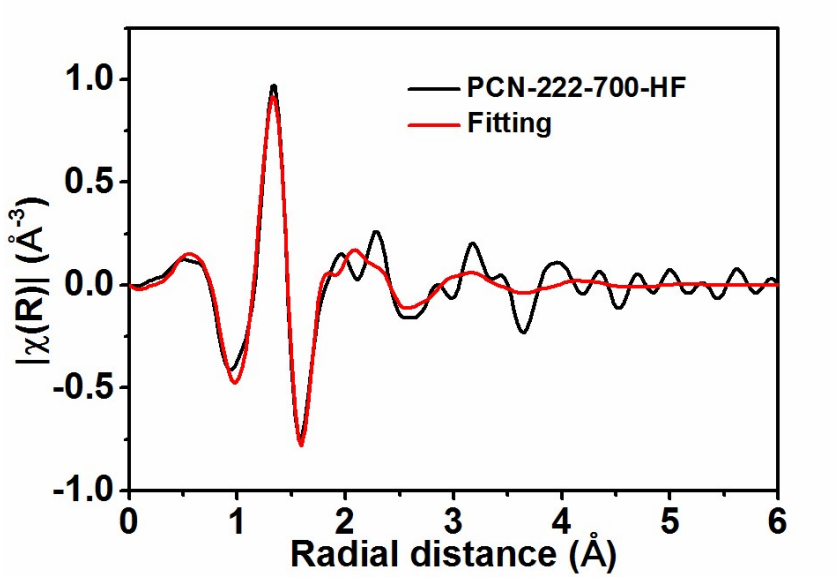

Figure S19. EXAFS R-space curve of PCN-222-700-HF with fitting.

Table S3. Fitting data of Fe K-edge EXAFS for PCN-222-700-HF

Sample	Coordination number	R (Å)	σ^2 (10^{-3} Å^2)	ΔE_0 (eV)
PCN-222-700-HF	6.0	1.94	8.0	-10.2

R(Å) denotes the distance between absorber and backscatter atoms; σ^2 is Debye-Waller factor for the description of the variance due to disorder (both lattice and thermal); ΔE_0 represents the inner potential correction.

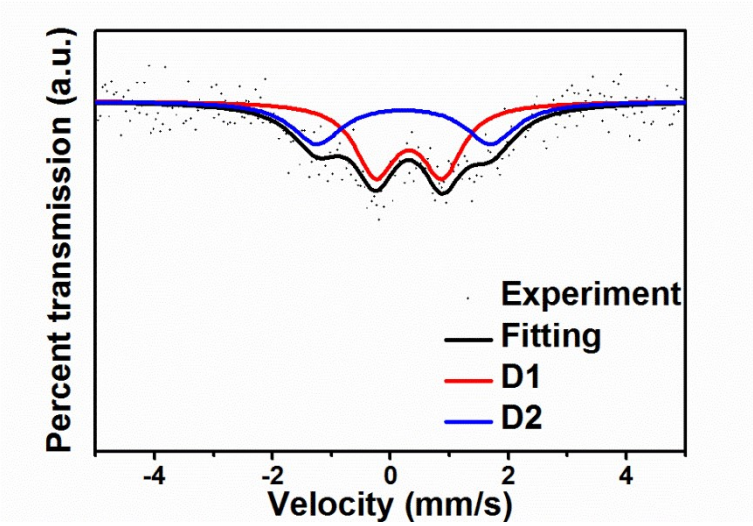

Figure S20. ^{57}Fe Mössbauer spectrum of PCN-222-700-HF with fitting.

Table S4. Mössbauer parameters of PCN-222-700-HF derived from fittings

Component	Isomer shift ($mm\ s^{-1}$)	Quadrupole splitting ($mm\ s^{-1}$)	Line width ($mm\ s^{-1}$)	Area (%)
D1	0.31	1.12	0.84	56.79
D2	0.23	2.94	1.05	43.21